INTERNATIONAL JOURNAL OF CIVIL ENGINEERING AND TECHNOLOGY (IJCIET)

ISSN 0976 – 6308 (Print)
ISSN 0976 – 6316(Online)
Volume 6, Issue 5, May (2015), pp. 85-99

Journal Impact Factor (2015): 9.1215 (Calculated by GISI)
www.jifactor.com

IJCIET

©IAEME

INTERFACIAL DELAMINATION FAILURE IN BONDED CONCRETE OVERLAY SYSTEMS - A REVIEW OF THEORIES AND MODELLING METHODS

Adegoke OmotayoOlubanwo[1], John Nicholas Karadelis[2]

[1,2]Department of Civil Engineering, Architecture and Building,
Coventry University, Priory Street, Coventry, United Kingdom, CV1 5FB

ABSTRACT

This study reviews the theories and modelling methods for describing interfacial delamination failure process between two bonded cementitious materials. Complex interfacial stress conditions at discontinuities and areas of high stress concentrations were primary areas of concern. Distinct analytical cases involving intrinsic material and structural property variables were considered. An approach based on plane strain analysis within the context of Interface Cohesive Zone Model (ICZM) was cited and presented as viable for describing and predicting delamination mode of failure in bonded concrete overlays systems (BCOs). The study shows that the use of numerical computational tools is vital in resolving the manifold complexity associated with interfacial delamination problems. In the concluding analytical model, it is evident that the numerical values of the delamination failure coefficient(D) and the corresponding Mixed-Mode energy release rates (G_{ic}) vary depending on the overlay structural scale, the type of problem (plane stress or plane strain) and the degree of mismatched properties between the overlay and the substrate.

Keyword: Interfacial, ICZM, Delamination, BCOs, Mismatched.

1.0 INTRODUCTION

Adequate interfacial bond performance of Bonded Concrete Overlays (BCOs) requires novel integration of material mixture design, compatibility model development, and robust interfacial bonding techniques. This whole process entails the use of the right material, on the right substrate, in the right way, in order to secure the best possible composite behaviour. In this respect, the structural integrity of pavement can be reinstated with enormous benefits, ranging from resource conservation to good returns on investment.

However, in spite of the plausible benefits accruing from BCO system of repair when compared to Un-bonded Concrete Overlay systems (UBCOs), early-age delamination problem

remains a bugging issue (Karadelis and Koutselas, 2003; Olubanwo, 2013). Hence, the doubt often arises as to whether the bond integrity of the BCO systems can be trusted, in particular at early-age, when the interface experiences strident self-equilibrated stresses resulting from both mismatched properties and differential length change effects.

Certainly, solving delamination problem requires a more pragmatic approach than just ensuring early interfacial bond development. Optimum solution often requires a holistic approach (Morgan, 1996; Emmons and Vaysburd, 1996) during which the thermo-mechanical compatibility and stability between the bonded layers are assessed and ascertained a priori. Implementing such tasks is non-trivial. Typically, it may involve bond optimization analysis using empirical and computational methods in order to assess and predict both early and long-term durability performance of the bonded system. Extensive review and work in this line has been presented elsewhere (Olubanwo and Karadelis, 2014).Until now, much of the optimization works for BCO system design revolves largely round thickness requirement. Fragmentary approach of this nature is somewhat insufficient and could result in abrupt material and subsequent structural failure of the BCOs (Olubanwo, 2013).In the literature, several successful interface models exist, not without drawbacks though. The following sections review and discuss briefly some prominent ones and their governing theories.

2.0 DELAMINATION MODEL DESCRIPTIONS

From experimental and analytical standpoints, two basic approaches are commonly used for simulating and describing the failure or de-bonding process of the interface– (1) stress-basedfailure criterion approach and (2) Energy-based fracture criterion approach. By definition, the two approaches defer in experimental concepts and computational techniques. For instance, in the limit analysis or the so-called stress-based approach, the interface is often assumed as perfectly bonded, while the classical energy-based method (Linear Elastic Fracture Mechanics - LEFM)treats the interface as having some well-established intrinsic defects.

However in quasi-brittle materials like concrete, the two extreme collapse methods cited above are rear and mostly infeasible; hence, more robust methods are desirable. In this paper, Interface Cohesive Zone Model (ICZM) within the concept of non-linear fracture mechanics is reviewed and proposed as a desirable alternative for describing the failure mechanism of concrete based interface. In the method, delamination process involving both crack initiation and propagation within a unified model is represented. The model treats delamination as progressive. Special cases of failure due to differential length change at discontinuities involving possible elastic mismatched conditions and structural scale properties are considered distinctly.

2.1 Traditional Stress-based approach

Essentially in stress-based approach, in order to ensure that the delamination process of the interface is adequately depicted, the mechanical characterization of the interface requires two basic descriptive states: (1) a state representing a perfectly bonded condition, and (2) a state defining delamination on set and propagation. In the former, adhesion between the bonded layers is assumed sufficiently strong; there by, imposing both stress and displacement continuity across the interface. In Shah and Stang (1996), the corresponding kinetics and the kinematics for continuity requirements at the interface are given by:

$$\left.\begin{aligned} \tau_{top} &= \tau_{btm} \\ \sigma_{top} &= \sigma_{btm} \\ u_{top} &= u_{btm} \\ v_{top} &= v_{btm} \end{aligned}\right\} \quad \text{on } I_b \qquad (2.1)$$

Where,$I_b$isall points on the bonded interface, τ and σ are respective shear and normal stresses of a point on the interface, while v and u are their corresponding tangential and normal displacements. Note, the subscripts 'top' and 'btm' represent the top and bottom layer respectively.

As seen, equation 2.1 lacks practicality in many instances, basically because it is premised on the assumption of a perfectly elastically bonded interface with no possibility of yielding or de-bonding. In reality, the interface yields or de-bonds at considerable lower stresses compared to adjacent bulk domains as stresses localize or concentrate in the plane of the interface due mainly to bond imperfection and mismatched elastic properties between the bonded materials. It has been shown that such localized or concentrated stresses can be three times more detrimental than the average stresses developing in the adjacent bonded materials (Kirsch, 1898; Dantu, 1958). Hence, characterizing the interface with a finite strength is commonplace in practice. Typically, for composite interface model of this nature, a general stress-based failure criterion takes the form:

$$F(\tau, \sigma, P_i) = 0 \qquad i = 1 \ldots, n \tag{2.2}$$

Where, $P_i$is one of n strength parameters, while other parameters are as given in equation 2.1.

From equation 2.2, the interfacial de-bonding process in limit analysis now permits the bonded interface to separate once it is loaded beyond its critical bond strength. The governing constitutive relations in this case are generally based on the kinematics of the interface, as the interface changes from its continuity condition to a prescribed surface traction boundary condition. In this case, the failure criterion takes the form (Shah and Stang, 1996):

$$\left.\begin{aligned} \tau_{top} &= \tau_{btm} = f \\ v_{top} &= v_{btm} = g \\ u_{top} - u_{btm} &\geq 0 \end{aligned}\right\} \text{ on } I_d \tag{2.3}$$

Where, I_d is all points on the de-bonded interface, while 'f' and 'g' are prescribed surface tractions in the general case. All other parameters are as given in equation 2.1.

Though the conditions given in equation (2.3) show a high explicit level about the nature of the de-bonding, the possibility of surface overlapping during de-bonding process is precluded; and often, this can be difficult to substantiate in reality, especially in cementitious materials where complicated interfacial contact problems dominate during de-bonding initiation stage (Shah and Stang, 1996).During subsequent steps, and at critical cracking stage of the interface, the interface attains a stress-free state (Atkinsonet al., 1982; Stang and Shah, 1986; and Morrison et al., 1988); hence, the frictional stress givenin equation (2.3) vanishes accordingly, so that it reads:

$$\left.\begin{aligned} \tau_{top} &= \tau_{btm} = 0 \\ v_{top} &= v_{btm} = 0 \end{aligned}\right\} \text{ on } I_d \tag{2.4}$$

If the interface is simultaneously influenced by stress and displacement continuities perpendicular to the interface, the boundary conditions given in equation (2.4) can be extended to include:

$$\left.\begin{aligned} \sigma_{top} &= \sigma_{btm} = 0 \\ u_{top} &= u_{btm} = 0 \end{aligned}\right\} \text{ on } I_d \tag{2.5}$$

Thus far, from engineering standpoint, the use of limit analysis as demonstrated above for both perfectly bonded and de-bonded interface surface characterization seems reasonable and

acceptable, but its inability to explain or capture the infinite stress condition at the crack-tip between the perfectly bonded region and the de-bonded zone of the interface remains a major drawback. The analytical proof of such stress singularities are based on complete linear elastic solution of the de-bonded interface problem. In the literature, it has been shown that the presence of these singularities is the reason why finite element analysis involving interface problem is mesh-dependent (Mormonieret al., 1988). In contrast, the justification of infinite stress state is also hard, if not impossible, if it is generally accepted that no material can be loaded beyond its yield strength. Consequently, it is inferred that many of the parameters employed in determining stress-based de-bonding criterion cannot be regarded as absolute material parameters, knowing that their values vary widely according to the type and complexity of the test and analysis used. Besides, it is likely - due to the incompleteness of the analysis - that the value of the strength parameters corresponding to a given interface will depend on the size, geometry and loading conditions of the composite system. Size effects, for instance, have been observed in similar tests, which, for instance, pure shear analysis fails to predict (Shah and Stang, 1996; Bazant and Zi, 2003). With the advent of modern computational tools, however, many of the problems associated with incomplete analysis or rigorous analytical solutions for de-bonded interface can be resolved.

2.2 Energy-based criterion

On the other hand, in energy-based criterion, methods based on classical Linear Elastic Interface Fracture Mechanics (LEIFM) have been found effective in describing and modelling crack propagation, particularly where material nonlinearities are negligible (Turon, et. al, 2004).As illustrated in Figure 2.1, for a bonded bi-material interface whose adjacent domains are characterized linearly by E_i, $\mu_i$and v_i for Young's Modulus, shear modulus, and Poisson's ratio of each domain respectively, it has been shown that there exists an intrinsic singularity with oscillatory field ahead of the crack tip (Williams, 1959), caused by the asymmetry in the elastic properties across the interface. This oscillatory field controls the measure of the competing or complex stress state near the crack-tip, which in terms of stress intensity factors can be expressed as:

$$\sigma_{yy} + i\tau_{xy} = \frac{(K_1 + iK_2)r^{i\varepsilon}}{\sqrt{(2\pi r)}} \qquad (2.6)$$

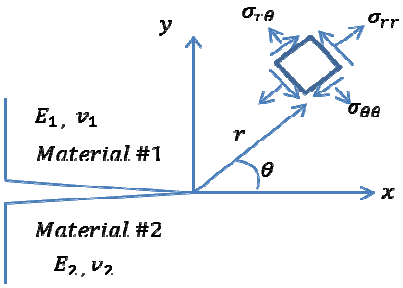

Figure 2.1: Linear crack along a Bi-material Interface

Where$r^{i\varepsilon} = \exp(i\varepsilon \log r) = \cos(\varepsilon \log r) + i \sin(\varepsilon \log r)$,$i = \sqrt{-1}$, r is the distance ahead of the crack-tip,ε is the oscillatory index defined later in equation (2.9), K_1 and K_2 are components of the complex stress intensity factor derived by Rice and Sih (1965) by solving the following logarithmic expressions which result from a full boundary-value problem of a given test specimen (Carlsson and Prasad, 1993; Chandra, 2002):

$$K_1 = \frac{\sigma[\cos(\varepsilon \log 2a)+2\varepsilon \sin(\varepsilon \log 2a)]+\{\tau[\sin(\varepsilon \log 2a)-2\varepsilon \cos(\varepsilon \log 2a)]\}}{\cosh \pi\varepsilon}\sqrt{a} \quad (2.7)$$

$$K_2 = \frac{\tau[\cos(\varepsilon \log 2a)+2\varepsilon \sin(\varepsilon \log 2a)]-\{\sigma[\sin(\varepsilon \log 2a)-2\varepsilon \cos(\varepsilon \log 2a)]\}}{\cosh \pi\varepsilon}\sqrt{a} \quad (2.8)$$

From where, εisestimated as:

$$\varepsilon = \frac{1}{2\pi} \text{In}\left[\frac{1-\beta}{1+\beta}\right] \quad (2.9)$$

In equation (2.9), (β)relates to one of Dundur's elastic mismatched parameters (Dundur, 1969) which measures the relative compressibility of the two bonded materials, commonly estimated from equation (2.10), say, for plane strain problems (Mei et. al, 2007); while its counterpart (α)given in equation (2.11) measures the corresponding relative stiffness (Mei et. al, 2007; Schmauder, 1990;Bower, 2010).

$$\beta = \frac{1}{2}\left[\frac{\mu_1(1-2v_2)-\mu_2(1-2v_1)}{\mu_1(1-v_2)+\mu_2(1+v_1)}\right] \quad (2.10a)$$

Which on simplifying yields:

$$\beta = \frac{E_1^{'}(1-v_1)(1-2v_2)-E_2^{'}(1-v_2)(1-2v_1)}{2(1-v_1)(1-v_2)(E_1^{'}+E_2^{'})} \quad (2.10b)$$

Where,$E_i^{'} = E_i/(1-v_i^2)$ *plain strain Young's Modulus for material i*

$$\alpha = \frac{E_1^{'}-E_2^{'}}{E_1^{'}+E_2^{'}} \quad (2.11)$$

Subsequently, under a Mixed-Mode fracture analysis, the energy release rate,(G), for crack extension per unit length along the interface for plain strain is generally given by (Carlsson and Prasad, 1993):

$$G = \frac{|K|^2}{E^* cosh^2 \pi\varepsilon} \quad (2.12)$$

Where,

$$|K| = \sqrt{K_1^2 + K_2^2} \quad (2.13)$$

$$cosh^2 \pi\varepsilon = 1/(1-\beta^2) \quad (2.14)$$

$$\frac{1}{E^*} = \frac{1}{2}\left(\frac{1}{E_1^{'}} + \frac{1}{E_2^{'}}\right) \quad (2.15)$$

Thus, by Mode-Mixity, the value of(G) as a function of the loading phase angle$(\acute{\Psi})$follows the real and imaginary stress intensity factors of the remote field lying ahead of the crack tip. This phase angle is typically expressed as:

$$\acute{\Psi} = tan^{-1}\left[\frac{Im(K_1+iK_2)L^{i\varepsilon}}{Re(K_1+iK_2)L^{i\varepsilon}}\right] \quad (2.16a)$$

Where, L is the arbitrary reference length selected to characterize the remote field. For most bi-material systems, it is clear that the value and the effect of nonzero (β) is small, and so in significant (Bower, 2010; Buyukozturk and Hearing 1998). Thus, by setting$\varepsilon = 0$, for most material combinations, equation 2.16asimplifies to:

$$\acute{\Psi} = tan^{-1}\left(\frac{K_2}{K_1}\right) \qquad (2.16b)$$

The corresponding displacement components behind the crack tip are given in Bower (2010) by:

$$d_y + id_x = \frac{4|K|e^{i\acute{\Psi}}}{E^*(1+2i\varepsilon)cosh\,(\pi\varepsilon)}\sqrt{\frac{r}{2\pi}}\left(\frac{r}{L}\right)^{i\varepsilon} \qquad (2.17)$$

From the above equations, it is clear that the asymptotic solution for the interface crack differs significantly from the corresponding solution for a homogenous solid, because the oscillatory character due to both stresses and displacements increases frequency as crack tip is approached; hence, making it difficult to discretize the remote loading. Besides, the crack planes are predicted overlapping near the crack-tip a priori, which perhaps is still less than clear in many practical instances (Bower, 2010).

As seen above, the application of LEIFM approach is attractive when considering crack propagation process particularly for brittle materials. Here, the critical fracture condition is assumed to have been reached when the energy release rate G equals the fracture toughness of the interface $G(\acute{\Psi})$; that is:

$$G = G(\acute{\Psi}) \qquad (2.18)$$

In many experimental instances, it has been shown (Suo and Hutchinson, 1989; Charalambideset. al., 1990) that this interface resistance to delamination increases rapidly with phase angle.

In essence, while both approaches described above provide some degree of analytical comfort; in reality, evidence of initial perfect interfacial bonding or the presence of initial interfacial crack, together with its location and size may be difficult to spot or substantiate in a cementitious bonded overlay composite system. It is therefore thinkable to seek an enhanced method, where both interfacial crack initiation and propagation processes are described within a unified model. Employing nonlinear Interface Cohesive Zone Models (ICZM) affords a common opportunity for simulating both interface crack nucleation and crack growth. The governing concepts are well-known and particularly suitable for representing adhesion and decohesion processes between dissimilar materials (Mei et al, 2010).

2.3 Interface Cohesive Zone Model (ICZM)

In the Interface Cohesive Zone Model (ICZM), the primary consequence of nonlinear fracture analysis is based on the assumption of a finite fracture (cohesive) zone existing in the vicinity and ahead of the crack-tip, following Dugdale (1960) and Barenblatt (1962) models. The models as depicted in Figure 2.2 show that the so-called stress singularity (infinite stress state) concept commonly associated with crack-tips in elasticity theory is unrealistic (Cornec, et al., 2003).

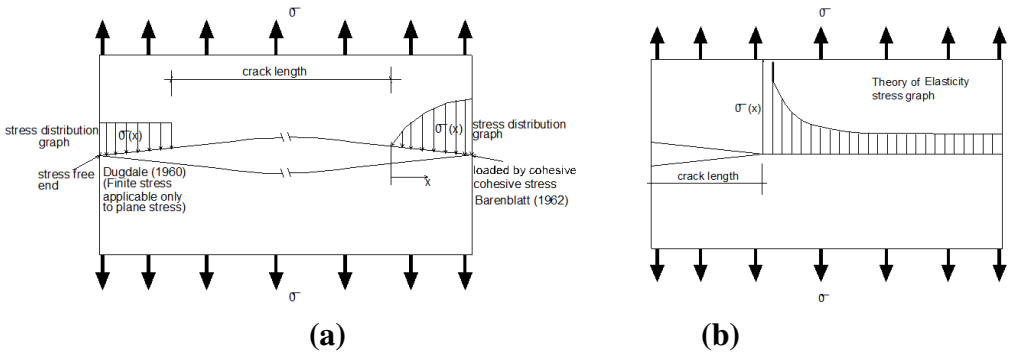

Figure 2.2: Comparison between (a) Dugdale and Barenblatt Models and (b) Stress singularity in Elasticity theory

The cohesive interface models represent a condition of a perfectly bonded interface undergoing de-bonding when the cohesive strength of the bonded interface varnishes with displacement discontinuity (Shah and Stang, 1996). Hence, for phenomenological nucleation and propagation descriptions, ICZM is most attractive; in particular in materials like concrete, where the non-linearity and the damage zone in the vicinity and ahead of the crack-tip cannot be neglected.

Typically, for a complete interface nonlinear fracture model description, the following are essential:

- The behaviour of the bulk materials, and
- The behaviour of the fracture zone, where conditions for crack formation and evolution are pre-defined along a known crack path.

In general, cementitious materials are classified as quasi-brittle. Besides, because cementitious materials exhibit little or no bulk dissipation, an isotropic linear elastic behaviour, characterized by elastic modulus (E) and Poisson's ratio (v), can be assumed. With respect to the fracture zone behaviour, a softening damage characteristic along the interface can be assumed based on the kinetics and kinematics relations defined in Figure 2.3c&d.

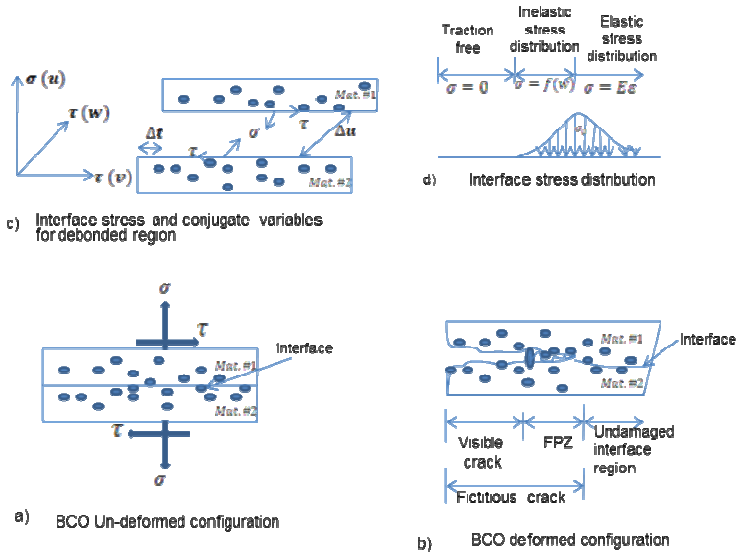

Figure 2.3: Interface configurations with Fracture Process Zone (FPZ) and Interface Stress Distribution

As seen, Figure 2.3 shows a BCO in its un-deformed and deformed configurations with a visible or true crack. The resulting FPZ, interface stress / conjugate variables, stress distribution curve between the FPZ and the elastic bi-material interface, and the constitutive relation defining each zone in the cohesive model after deformation are equally depicted. The overall cohesive model illustrated here follows the assumptions given below:

- The FPZ along the interface localizes into a single line ahead of the crack tip, with no possibility of kinking.
- The FPZ or the fictitious crack length is assumed mostly dominated by inelastic deformation.
- The materials lying adjacent the fictitious crack behave linearly elastic.
- The constitutive law governing the inelastic deformation at the FPZ assumes stress-displacement relationship.

  In this respect, the associated kinematics in this sense refers to the relative motion of the two deformed layers at the interface and may be described as:
- In Figure 2.3(c), u represents a unit vector in normal direction to the interface.
- At the interface, two mutual tangential unit vectors,$\boldsymbol{v}$and $\boldsymbol{w}$,are introduced.
- But for cementitious inter face where isotropic condition applies, the tangential deformation along $\boldsymbol{v}$ and $\boldsymbol{w}$ directions is treated as equal. Hence, the constitutive relation can be defined in terms of scalar Cartesian components $\Delta\boldsymbol{u}$ and $\Delta\boldsymbol{t}$ only (Bower, 2010), which represent the relative displacements of two initially coincident points at the interface, in normal and tangential directions respectively. (Where: $\Delta\boldsymbol{t} = \sqrt{\boldsymbol{v}^{2+}\boldsymbol{w}^{2}}$).

The kinetics relate to the forces acting between the two contacting layers. In this case, the two equal and opposite tractions are assumed acting on two initially coinciding points before and during interface deformation. Thus, under isotropic condition, the corresponding interface tractions are given by the scalar components $\boldsymbol{T_n}$ and $\boldsymbol{T_t}$in thenormal and tangential plane respectively.

3.0 APPLICATIONS OF INTERFACE COHESIVE ZONE MODEL TO CONCRETE

The use of finite cohesive zone for cementitious materials is well-known, following the linear softening model of Hillerborget al. (1976). The application of cohesive zone model (CZM) for cementitious materials has since grown into popularity due to its computational convenience, and it is probably the best fracture model for simulating fracture processes in cementitious materials and structures (Bazant, et al., 2002).

Interestingly, for concrete, both linear softening model, introduced by Hillerborget al. (1976), and bilinear softening model, developed by Petersson (1981), can be implemented. With most Finite Elementcodes, the surface traction can easily be obtained as an extrapolation of standard Gauss nodal stresses between adjacent continuum interface elements.

For instance, in ANSYS FE software, the contacting interface can be modelled as a zero-thickness contact plane characterized with associative cohesive elements with constitutive properties along a pre-defined interface between two adjacent continuum elements and the resulting interfacial damage initiation and evolution defined by the nonlinear traction-separation (bi-linear) law described in Alfano and Crisfield(2001).

As shown in Figure 3.1, the interface in a bi-linear model is assumed to behave elastically under deformation with initial stiffness (k_0) until the applied stress reaches the cohesive strength (σ_0) of the interface, at which point the damage initiation occurs. It should be noted that the initial elastic stiffness (k_0) has a character of a penalty factor only rather than a physical stiffness, hence it is discretionary kept high to ensure minimum elastic deformations of the interface (i.e. of negligible degree), so as to minimise interpenetration, separation or sliding prior to cracking.

International Journal of Civil Engineering and Technology (IJCIET), ISSN 0976 – 6308 (Print), ISSN 0976 – 6316(Online), Volume 6, Issue 5, May (2015), pp. 85-99 © IAEME

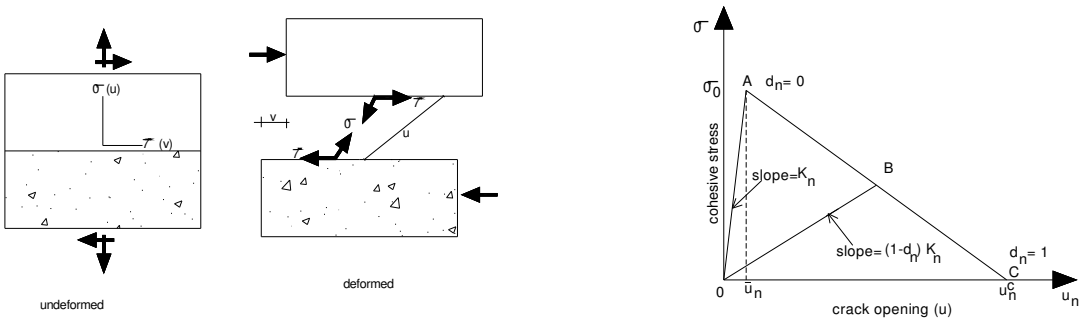

(a) **(b)**

Figure 3.1: a) Definition of stress and conjugate variables, and b) Bilinear softening relation

As seen in Figure 3.1, the delamination process is defined by two slopes OA and AC. The initial slope OA represents the linear elastic regime of the curve, while the second slope defines the softening part of the curve in a linear function. De-bonding is assumed to initiate at peak contact stress (σ_0) at point A, and grows linearly as a function of de-bonding parameter (d). The value of (d) evolves progressively from 0 to 1based on the conditions shown in equation 3.1till all the interface stresses reduce to zero at critical crack point C (u_n^c).

$$d = \begin{cases} 0 & for \;\; u_n = \bar{u}_n \\ 0 < d \leq 1 & for \;\; u_n > \bar{u}_n \end{cases} \tag{3.1}$$

Where,

$u_n = separation\ of\ the\ interface\ elements\ over\ the\ entire\ loading\ history.$
$\overline{u}_n = \frac{\sigma_0}{k_0} = critical\ separation\ for\ damage\ initiation$
$\sigma_0 = cohesive\ strength$
$k_0 = initial\ elastic\ contact\ stiffness$

Thus, for each mode of failure during loading, the fracture cohesive stress (T) can be related to the opening or sliding displacement linearly by:

$$T = \begin{cases} \sigma = k_n u_n (1 - d_n) & for \;\; Mode\ I \\ \tau = k_t u_t (1 - d_t) & for \;\; Mode\ II \end{cases} \tag{3.2}$$

Where, σ and τ are the cohesive stresses in the normal and tangential directions respectively, whilek_n and k_t denote the corresponding contact stiffnesses. $u_n$andu_t represent the accompany displacements after deformation,while d_n and d_t are the resulting de-bonding parameters in Mode I and Mode II respectively.

However, for bonded dissimilar materials, Mixed-Mode delamination is common during loading and failure process, thus, the criteria for damage initiation and final failure must account for the concomitant effects of Mode I and Mode II. In that respect, both normal and tangential traction-separation curves can be expanded in the ($u_n\ and\ u_t$) - plane, as illustrated in Figure 3.2.From here, it is clear that the normal and shear stresses depend not only on their corresponding displacement, but on both the shear slip and normal opening as given in equation 3.3:

$$\left.\begin{matrix}\sigma\,(u_n,\,u_t)\\ \tau\,(u_n,\,u_t)\end{matrix}\right\} \tag{3.3}$$

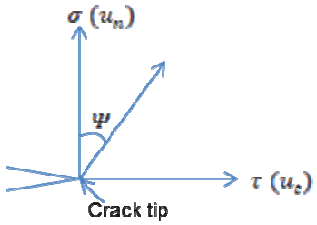

Figure 3.2: Mixed-Mode oscillatory field at crack-tip

Consequently, the effective traction vector and the corresponding effective displacement can respectively be expressed as:

$$\lambda_m = \sqrt{\langle\sigma\rangle^2 + \tau^2} = \frac{\langle\sigma\rangle}{Cos\,\Psi} = \frac{\tau}{Sin\,\Psi} \tag{3.4}$$

$$u_m = \sqrt{\langle u_n\rangle^2 + {u_t}^2} = \frac{\langle u_n\rangle}{Cos\,\Psi} = \frac{u_t}{Sin\,\Psi} \tag{3.5}$$

Thus, for a local Mixed-Mode fracture, the critical magnitude of the traction vector now depends on the ratio between the shear and normal tractions, which by definition is the phase angle given in equation 3.6.

$$\Psi = tan^{-1}\left(\frac{\tau}{\langle\sigma\rangle}\right) \tag{3.6}$$

In effect, as Ψ increases, the normal stress-crack opening curve diminishes from $\Psi = 0^0$, while the shear stress-sliding curve expands towards a maximum for $\Psi = 90^0$.

It should be noted that the phase angle (Ψ) defined here can be at variance from the global phase angle ($\acute{\Psi}$) defined earlier in equation (2.16b) for the LEIFM, though they both measure the relative proportion of the effect of Mode II fracture to Mode I fracture on the interface. For many practical systems (Buyukozturk and Hearing, 1998), including cementitious interface, the effect of non-zero (β) is of secondary consequence; hence, the global phase angle can conveniently be reduced to $\acute{\Psi} = arctan\left(\frac{K_{II}}{K_I}\right)$as shown earlier.

Therefore, since the phase angle given by equation 3.6 is of local Mixed-Mode effect, its numerical value may vary along the interface - from element to element – (Mei et al, 2010);its degree of variation with respect to delamination length is however expected to be relatively insignificant for short crack limit where delamination length (l_d) is less that the overlay thickness ($h_{overlay}$). Hence, it is appropriate to assume a constant steady-state phase angle during the analysis, while treating the interface toughness as independent of the delamination length, but a dependent function of the phase angle, so that the interface attains its critical fracture condition when the Mixed-Mode energy release rate G_{ic} equals the fracture toughness of the interface $G_{ic}(\Psi)$ as given in equation 3.9:

$$G_{ic} = G_{ic}(\Psi) \tag{3.9}$$

The expression given here is similar to the one given in equation 2.18, except that the value of (Ψ) is local while that of ($\acute{\Psi}$) is global.

4.0 DELAMINATION MODEL FOR DIFFERENTIAL LENGTH CHANGE AT DISCONTINUITIES

Consider a finite bonded concrete overlay system shown in Figure (4.1a) resting on elastic foundation, and experiencing a differential length change, either due to thermal gradient or drying shrinkage of the overlay. The curling effects of the uniaxial edge-stress condition, say for contraction, can be idealized as shown in Figure (4.1b) such that stresses are assumed as acting on a beam at the edges rather than on the entire slab surface (Houben, 2006). With increased deformation concentrating at the top edge surface of the overlay during the curling process, a partial (l_{cz}) or true interface delamination length (l_d) may be induced along the edges. Apparently, for Mixed-Mode delamination to occur, the failure condition given in equation 3.9 must be satisfied.

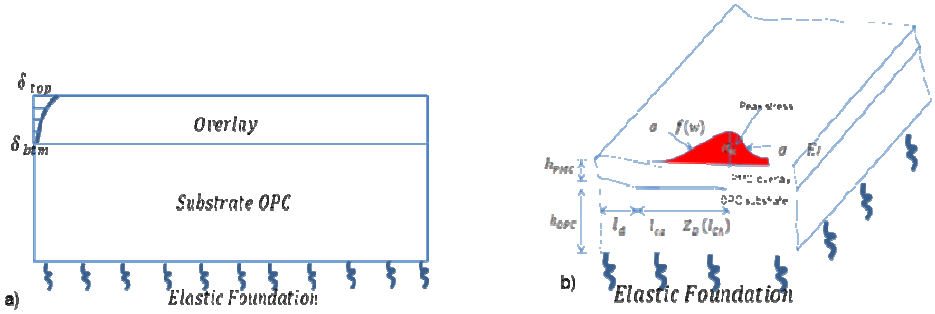

Figure 4.1: Overlay Edge Deformation and Delamination

From the idealized model shown in Figure 4.1, a 2D plane strain analysis can be implemented to estimate the magnitude of the interface delamination driving energy as a function of the overlay structural scale and elastic mismatched properties of the bi-material. The structural scale corresponds to the ratio of the prescribed overlay thickness to the total thickness of the BCO system in order to keep the scale dimensionless. The mismatched elastic properties are controlled by Dundur's parameters given in equations 2.10 and 2.11.

From here, three distinct variables can be associated with the delamination function (D) based on the expression given in equation 4.1.

$$D = f\left(\frac{h_{overlay}}{h_{total}}, \alpha, \beta\right) \tag{4.1}$$

From equation 4.1, the first parameter in the bracket $\left(\frac{h_{overlay}}{h_{total}}\right)$ denotesthe structural scale, and often helps to investigate the thickness response of the overlay to delamination when one of the two Dundur's parameters is fixed. In most applications, the limiting value of $h_{overlay}$ falls between 50 and 125mm. For reasons given earlier, the effect of non-zero (β) is secondary and subsequently can be held fixed for all possible material combinations. Thus, in order to estimate the FPZ (l_{cz}) along the interface, the following relationship holds (Gdoutos, 2005):

$$l_{cz} = D\,(l_{Ch}) = D\left(\frac{E^* G_{Fm}}{\lambda_m^2}\right) \tag{4.2}$$

Where, D is as defined in equation 4.1, l_{Ch} is Hillerborg's characteristic length defined by $\left(\frac{E^* G_{Fm}}{\lambda_m^2}\right)$,$E^* = average\ elastic\ modulus\ of\ the\ bi-material\ (same\ as\ equation\ 2.15)$,$\lambda_m = effective\ traction\ for\ mixed\ mode\ damage\ initiation\ (same\ as\ equation\ 3.4)$,
$G_{Fm} = Mixed-Mode\ fracture\ energy = G_I + G_{II}$
$G_I = Mode\ I\ fracture\ energy = \frac{1}{2}\lambda_m u_m^c cos^2\Psi$(4.3)
$G_{II} = Mode\ II\ fracture\ energy = \frac{1}{2}\lambda_m u_m^c sin^2\Psi$(4.4)
$u_m^c = critical\ (effective\ )\ mixed\ mode\ dis[lacement$

If the Mixed-Mode delamination criterion is specified in terms of fracture energy, equations 4.5 and 4.6 hold:

$$\left(\frac{G_I}{G_{Ic}}\right) + \left(\frac{G_{II}}{G_{IIc}}\right) = 1 \quad (4.5)$$

$$\text{Since, } G_{Fm} = G_{Ic} + G_{IIc} = \frac{1}{2}\lambda_m u_m^c = G_{Ic}\left[cos^2\Psi + \frac{G_{Ic}}{G_{IIc}} sin^2\Psi\right]^{-1} \quad (4.6)$$

Where, $G_{Fm} = fracture\ toughness\ or\ critical\ fracture\ enegy\ for\ Mixed-Mode$
$G_{Ic} = Fracture\ toughness\ or\ critical\ fracture\ energy\ in\ pure\ mode\ I$
$G_{IIc} = Fracture\ toughness\ or\ critical\ fracture\ energy\ in\ pure\ mode\ II$

Rearranging equation 4.2 and expressing the resulting energy release rate in terms of the overlay structuralsize, equation 4.7obtains:

$$G_{F^m} = D\left(\frac{h_{overlay}}{h_{total}}, \alpha, \beta\right) \frac{\lambda_m^2 h_{overlay}}{E^*} \quad (4.7)$$

With respect to equation 3.9, the delamination failure definition given in equation 4.7 can further be expressed as a function of the normalized interface toughness such that:

$$G_{ic} = D\left(\frac{h_{overlay}}{h_{total}}, \alpha, \beta\right) = \frac{E^*\, G_{ic}(\Psi)}{\lambda_m^2 h_{overlay}} \quad (4.8)$$

In this respect, the delamination failure coefficient(D) can be numerically estimated as a function of the normalized structural scale for different values of (α). This approach relates to plane strain problems and similar model has been presented elsewhere (Mei et al, 2010), though with a structural scale adjustment. In the literature, several values of (D)based on plane stress problems also exist and they are reported in Turon, et. al.(2007). As illustrated in Table 4.1, such values range between 0.21 and 1.0; though Hillerborg's and Rice's models where values of (D) approach or equal to unityare mostcommon in practice.

Table 4.1: Cohesive zone length and equivalent delamination dimensionless parameter

$Model$	l_{cz}	D
Hui	$2/3\pi\,.E\,Gc/{\lambda_{cm}}^2$	0.21
Irwin	$1/\pi\,.E\,Gc/{\lambda_{cm}}^2$	0.31
Dugdale, Barenblatt	$\pi/8\,.E\,Gc/{\lambda_{cm}}^2$	0.40
Rice, Falk	$9\pi/32\,.E\,Gc/{\lambda_{cm}}^2$	0.88
Hillerborg	$E\,Gc/{\lambda_{cm}}^2$	1.00

Evidently, from Table 4.1, there exists no unified value of (D)per se. By inspection, the values of(D)will depend on the overlay structural scale, the type of problem (plane stress or plane strain), the method and the magnitude of loading, and the degree of mismatched elastic properties between the overlay and the substrate.

5.0 CONCLUSIONS

The research showed that for a composite Bonded Concrete Overlay system, the use of numerical computational tools is vital considering the level of complexity involved in determining the effects of intrinsic structural and mismatched material properties on interfacial delamination. An approach based on plane strain analysis within the context of Interface Cohesive Zone Model has been presentedas viable for simulating and predicting delamination mode of failure in BCO systems. From the information given in this paper, the following can be concluded:

- Many of the drawbacks associated with stress-based approach and classical energy-based method (LEIFM) such as size effects, incomplete computational analysis and stress singularities are overcome in the nonlinear interface fracture mechanics (NLIFM) approach.
- A unified model where both interfacial crack nucleation and propagation processes are present can be implemented using nonlinear interface fracture mechanics approach.
- The numerical values of delamination failure coefficient(D) and Mixed-Mode energy release rates (G_{ic}) can vary depending on the overlay structural scale, the type of problem (plane stress or plane strain), the method and the magnitude of loading, and the degree of elastic mismatched properties between the overlay and the substrate.

ACKNOWLEDGMENTS

The authors gratefully acknowledge the financial support of Aggregate Industries, UK.

REFERENCES

1. Alfano, G. and Crisfield, M.A. (2001) “Finite Element Interface Models for the Delamination Anaylsis of Laminated Composites: Mechanical and Computational Issues,” International Journal for Numerical Methods in Engineering, 501701-1736.
2. Atkinson, C., Avila, J., Betz, E. and Smelser, R.E. (1982) “The rod pull out problem, theory and experiment,” Journal of Mechanics and Physics of Solids, 30, 97 – 120.
3. Barenblatt, G. I. (1962), “The Mathematical theory of equilibrium cracks in brittle fracture,” Advanced Applied Mechanics, 7, 55–129.
4. Bazant, Z. P., Yu, Q., and Zi, G. (2002) “Choice of standard fracture test for concrete and its statistical evaluation,” International Journal of Fracture, 118, 303 – 337.
5. Bazant, Z. P. and Zi, G. (2003) “Size effect law and fracture mechanics of the triggering of dry snow slab avalanches,” Journal of Geophysical research, **108**(B2), 2119.
6. Bower, A.F. (2010) Applied Mechanics of Solid, Taylor and Francis Group, LLC.
7. Buyukozturk O. and Hearing, B. (1998) “Crack propagation in concrete composites influenced by interface fracture parameters,” International Journal of Solids and Structures, **35**(31-32) 4055 – 4066.
8. Carlsson, L.A. and Prasad, S., (1993) “Interfacial fracture of sandwich beams,” Engineering Fracture Mechanics, 44(4) 581 – 590.
9. Chandra, N. (2002) “Evaluation of interfacial fracture toughness using cohesive zone model,” Composite: Applied science and manufacturing, Part A 33, 1433 – 1447.

10. Charalambides, P. G., Cao, H.C. Lund, J. Evans, A.G. "Development of a test method for measuring the mixed mode fracture resistance of bimaterial interfaces," Mechanics of Materials, 8, 269 – 283 (1990).
11. Cornec, A., Scheider, I. and Schwalbe, K. (2003) "On the practical application of the cohesive model," Engineering Fracture Mechanics, **70**(14), 1963-1987.
12. Dantu, P. (1958) "Study of the distribution of stresses in a two-component heterogeneous medium. Symposium Non-Homogeneity in Elasticity and Plasticity," Warsaw. Pergamon Press, London, pp. 443 – 451.
13. Dugdale, D.S. (1960) "Yielding of steel sheets containing slits," Journal of the Mechanics and Physics of Solids, 8, 100- 104.
14. Dundurs, J. (1969) "Edge-Bonded Dissimilar Orthogonal Elastic Wedges Under Normal and Shear Loading," ASME Journal of Applied Mechanics, 36, 650 – 652.
15. Emmons, P.H. and Vaysburd, A.M. (1996) "System concept in design and construction of durable concrete repairs," Construction and Building Materials, **10** (1), 69 – 75.
16. Falk, M.L., Needleman, A., Rice J.R. (2001) "A critical evaluation of cohesive zone models of dynamic fracture," Journal de Physique IV, Proceedings, 543-550.
17. Gdoutos, E.E. (2005) Fracture Mechanics: An Introduction, 2nd edn. Springer.
18. Hillerborg, A., Modeer, M. and Petersson, P.E. (1976) "Analysis of crack formation and crack growth in concrete by means of fracture mechanics and finite elements," Cement and Concrete Research, 6, 773 – 782.
19. Houben, L. J. M. (2003) "Structural design of Pavement – Part IV: Design of Concrete Pavements, Lecture Notes CT4860," Faculty of Civil Engineering and Geosciences, TU Delft; Delft.
20. Hui, C.Y., Jagota, A., Bennison, S.J., Londono, J.D. (2003) "Crack blunting and the strength of soft elastic solids," Proceedings of the Royal Society of London A, 459, 1489-1516.
21. Irwin, G.R. (1960) "Plastic zone near a crack and fracture toughness. In Proceedings of the Seventh Sagamore Ordnance Materials Conference," vol. IV, 63-78, NewYork: Syracuse University.
22. Karadelis, N.K. and Koutselas, K. (2003) "Sustainable 'Green' Overlays for Strengthening and Rehabilitation of Concrete Pavements. In: Proceedings, 10th International Conference, Structural Faults + Repair," London, UK, ISBN 0-947644-52-0, 94 (also on CD-ROM).
23. Kirsch, (1898) Die Theorie der Elastizität und die Bedürfnisse der Festigkeitslehre. Zeitschrift des Vereines deutscher Ingenieure, 42, 797–807.
24. Mei, H., Pang, Y. and Huang, R. (2007) "Influence of Interfacial delamination on Channel cracking of elastic thin-films," Int. Journal of Fracture, 148, 331 – 342.
25. Mei, H., Gowrishankar, S., Liechti, K.M. and Huang, R. Initial and Propagation of interfacial delamination integrated thin-film structureshttp://www.utexas.academia.edu /ShravanGowrishankar [12November 2010].
26. Morgan, D.R. (1996) "Compatibility of concrete repair materials and systems," Construction and Building Material, 10, No.1, 57-67.
27. Mormonier, M.F., Desarmot, G., Barbier, B. and Letalenet, J.M. (1988) "A study of the pull-out test by a finite element method (in French)," Journal of Theoretical and Applied Mechanics, 7, 741 – 765.
28. Morrison, J.K., Shah, S.P. and Jena, Y.S. (1988) "Analysis of fibre debonding and pullout in composites," ASCE Journal of Engineering Mechanics, **114**(2), 277 – 294.
29. Olubanwo A.O. (2013) "Optimum design for Sustainable 'Green' Bonded Concrete Overlays: Failure due to shear and delamination."PhD Thesis, Department of Civil Engineering, Architecture, and Building Coventry University, United Kingdom.

30. Olubanwo, A.O. and Karadelis, N. K. (2014) "Applied mixture optimization techniques for paste design of bonded roller-compacted fibre reinforced polymer modified concrete (BRCFRPMC) overlays," RILEMJournal of Materials and Structure, DOI 10.1617/s11527-014-0291-x (Online First ed.)
31. Petersson, P.E. (1981) "Crack Growth and Development of Fracture Zones in Plain Concrete and Similar Materials," Report TVBM – 1006, Division of Building Materials, Lund Inst. of Technology, Lund, Sweden.
32. Rice, J. R. and Sih, G. C. 'Plane problems of cracks in dissimilar media.' Journal of Applied Mechanics, 418-423 (1965).
33. Schmauder, S. "Theory of the Elastic Interface Crack", Fortschrittsberichte der DeutschenKeramischenGesellschaft: Werkstoffe, Verfahren, Anwendung 1986/1987, Beiheftzu CFI (Ceramic Forum International) **2**, pp. 101-108 (1987).
34. Shah, H. and Stang, S.P. (1996) Micromechanics of interface in fibe-reinforced cement materials.In: Maso J.C. ed. Interfacial Transition Zone in Concrete, RILEM REPORT 11.E & FN SPON, 75 – 100.
35. Shah, H. and Stang, S.P. (1986) Failure of fibre-reinforced composites by pullout fracture.Journal of Materials Science, **21**(3), 953 -957.
36. Suo, Z.andHutchinson**,** J. W. "Sandwich specimens for measuring interface crack toughness,"Materials Science and Engineering**,** A107**,** 135-143(1989).
37. Turon, A., Davila C.G., Camanho P.P., Costa, J. "An Interface Damage Model for the Simulation of Delamination Under Variable-Mode Ratio in Composite Materials", National Aeronautics and Space Administration, NASA/TM-2004-213277, (2004), WASHINGTON, DC, USA.
38. Turon, A., Davila C.G., Camanho P.P., Costa, J. (2007) "An Engineering Solution for Mesh Size Effects in the Simulation of Delamination Using Cohesive Zone Models," Engineering Fracture Mechanics, 74, 1665–1682.
39. Williams, M. L. "The stresses around a fault or crack in dissimilar media." Bulletin of the Seismological Society of America, 49(2), 199-204 (1959).
40. Prerna Nautiyal, Saurabh Singh and Geeta Batham, "A Comparative Study of The Effect of Infill Walls on Seismic Performance of Reinforced Concrete Buildings" International Journal of Civil Engineering & Technology (IJCIET), Volume 4, Issue 4, 2013, pp. 208 - 218, ISSN Print: 0976 – 6308, ISSN Online: 0976 – 6316.
41. Vima Velayudhan Ithikkat and Dipu V S, "Analytical Studies on Concrete Filled Steel Tubes" International Journal of Civil Engineering & Technology (IJCIET), Volume 5, Issue 12, 2014, pp. 208 - 218, ISSN Print: 0976 – 6308, ISSN Online: 0976 – 6316.
42. Ananya John, Unni Kartha G. and Prof. S.Usha, "Analytical Study on Stress-Strain Behaviour of Reinforced Concrete Column" International Journal of Civil Engineering & Technology (IJCIET), Volume 5, Issue 12, 2014, pp. 45 - 55, ISSN Print: 0976 – 6308, ISSN Online: 0976 – 6316.